

OPTIMIZATION OF LASER CUTTING PARAMETERS FOR RECOMBINANT BAMBOO BASED ON RESPONSE SURFACE METHODOLOGY

RONGRONG LI, XIAOLEI GUO, PINGXIANG CAO
NANJING FORESTRY UNIVERSITY, FACULTY OF MATERIAL SCIENCE
AND ENGINEERING
NANJING, JIANGSU, CHINA

XIAODONG (ALICE) WANG
LULEÅ UNIVERSITY OF TECHNOLOGY, DIVISION OF WOOD SCIENCE
AND ENGINEERING
SKELLEFTEÅ, SWEDEN

(RECEIVED SEPTEMBER 2015)

ABSTRACT

A means for selecting the optimal process parameters for the laser cutting of recombinant bamboo, based on the design of experiments (DOE) approach, was presented. Recombinant bamboo with thicknesses of 5, 10, and 15 mm was cut by a CO₂ laser. The parameters investigated were the laser power, air pressure, and cutting speed. The results were compared using a number of process responses which define the efficiency of the cutting, including the upper kerf (UK) width, lower kerf (LK) width, and the ratio of upper-to-lower kerfs. Mathematical models were developed to establish the relationship between the process parameters and response parameters; special graphs were drawn for this purpose. Finally, a numerical optimization was performed to find out the optimal process settings to achieve a minimum upper-to-lower kerf ratio.

KEYWORDS: Recombinant bamboo, CO₂ laser cutting, design of experiment, optimization.

INTRODUCTION

Recombinant bamboo is a new type of engineered timber characterized by great structural integrity, high dimensional stability, good mechanical properties, and a density similar to that of hardwood (Wang and Hua 1991). It is made from bamboo via defibering, drying, gluing, laying-up, and hot-pressing (Zhao and Yu 2002). It is suitable for many interior construction and industrial applications. Unfortunately, the advantages of recombinant bamboo can also

complicate its processing, such as higher cutting temperature, tool wear, cutting force, and noise. Therefore, finding a suitable cutting method for recombinant bamboo is essential (Yang 2005).

At present, laser cutting has been a widely used processing method. A variety of materials, such as metals, plastics, rubbers, wood, ceramics, and composites can be cut, welded, and surface-treated by different types of lasers of different operating powers. Some studies have been published regarding the laser cutting of different materials, including stainless steel and plastics, analysing the effects of different laser beam cutting (LBC) parameters on the quality and characteristics of the cutting. In about 1970s, laser cutting has been concerned by some researchers in wood processing field. These researchers found laser cutting has about two advantages, one is its high precision, and the other is no tool wear, low noise emission and narrow kerf width (Mukherjee et al. 1990; Barcikowski et al. 2006; Naderi et al. 1990; Guo 2014a, b). In this research, CO₂ laser was applied to cut the samples, because of CO₂ gas wavelength and correspondent energy density that provide a high quality of cutting (Eltawahni et al. 2013).

Previous research has unveiled some of the relationships between process parameters (such as laser power, cutting speed, air pressure, and the focal plane position) and the characteristics of the CO₂ lasers cutting. And the water content, specific gravity, direction of cut, and thickness of the wood also greatly affect the speed of cutting (Pires et al. 1989; McMillin et al. 1971). The optimal cutting of medium-density fiberboard (MDF) and plywood is achieved by the combination of laser power, cutting speed, air pressure, and focal point position which yields high-quality process output at a low cutting cost (Eltawahni et al. 2011, 2013). The factors affecting the ability of lasers to cut wood may be generally classified into three categories: characteristics of the laser beam, equipment and process variables, and the properties of the work piece (Barnekov et al. 1986).

The purpose of this study was to investigate the effect of CO₂ laser cutting process parameters on the upper kerf (UK), lower kerf (LK), and the ratio between them and tried to determine reasonable process parameters for the cutting of recombinant bamboo. Normally, narrow kerf width and little ratio are desired as an ideal kerf in cutting process. An appropriate response surface methodology (RSM) technique was used, aiming to achieve the desired quality attributes. Desirable or optimal cutting conditions can be obtained by using the desirability approach and the models developed in this study.

MATERIAL AND METHODS

Materials and laser machine

Recombinant bamboo samples with thicknesses of 5, 10, and 15 mm were used as the work pieces. The recombinant bamboo was supplied by the Hunan Taohuajiang Industries Company, Ltd. The mechanical properties were determined in a three-point bending mode at a cross head speed of 10 mm·min⁻¹ with a span of 320 mm. The specimen size for mechanical property testing was 500 mm (L) × 30 mm (W) × 20 mm (T). Tab. 1 summarizes the mechanical and physical properties of the recombinant bamboo. Samples of dimensions of 100 mm (L) × 100 mm (W) were prepared for laser-cutting experiments.

The experiments were performed with a 3-kW CO₂ laser machine provided by the Shanghai Unity-prima Company. In this study, compressed air was used to remove the smoke and fumes generated by the laser-cutting operation. As reported in a previous study, there is no significant reduction in kerf width when using compressed air or nitrogen (Lum et al. 2000). The nozzle used has a conical shape with nozzle diameter of 1.5 mm. The upper and lower kerf width “responses” were measured using an optical microscope equipped with 0.1-μm-precision digital micrometers.

Tab. 1: The mechanical and physical properties of recombinant bamboo.

Material	Moisture content (%)	Density $\text{kg}\cdot\text{m}^{-3}$	Bending modulus of elasticity (GPa)	Bending strength (MPa)
Recombinant Bamboo	10 %	1050	25.2	257

Methods

In this study, response surface methodology (RSM) by the Box-Behnken design (a three-level design) was used. This design allows for ample investigation of the process with a relatively small number of runs as compared to the central composite design. It characterizes factors within the same operative and study regions, which allows for evaluation of each factor over its entire range. The experimental data was analyzed by statistical software (Design-Expert V8.0.6).

Plan of the experiment

Three parameters (laser power, air pressure, and cutting speed) were varied during the tests. First, the best ranges for these parameters were found by single-factor experimentation. Then, the RSM design was applied to optimize the parameters. Tab. 2 indicates the factors studied and the assignment of the corresponding levels. The term "level" refers to the factor values tested. The focal plane was set on the upper surface of the samples in all experiments.

Tab. 2: Process variables and experimental design levels.

Parameters	Code	Dimensions	Level								
			-1			0			1		
			Thickness (mm)			Thickness (mm)			Thickness (mm)		
			5	10	15	5	10	15	5	10	15
Laser power	A	W	500	1100	1400	700	1300	1700	900	1500	2000
Air pressure	B	bar	4.5	7	7	5.5	9	9	6.5	11	11
Cutting speed	C	$\text{m}\cdot\text{min}^{-1}$	2.5	2.5	2.5	3.5	3.5	3.5	4.5	4.5	4.5

RESULTS AND DISCUSSION

The outputs of the experiments and the average measured responses for each thickness are presented in Tabs. 3, 4, and 5. The upper and lower kerf values were measured by an optical microscope as discussed above.

Tab. 3: Design matrix and experimentally recorded data for 5 mm thickness.

Standard ^a	Run ^b	Factors			Responses		
		A (W)	B (bar)	C ($\text{m}\cdot\text{min}^{-1}$)	Upper Kerf (μm)	Lower Kerf (μm)	Ratio
1	8	500	4.5	3.5	113.5	73.2	1.55
2	13	900	4.5	3.5	164.6	121.9	1.35
3	15	500	6.5	3.5	118.4	81.1	1.46
4	14	900	6.5	3.5	170.1	131.9	1.29
5	10	500	5.5	2.5	141.9	102.8	1.38

6	6	900	5.5	2.5	192.4	161.7	1.19
7	1	500	5.5	4.5	125.6	85.4	1.47
8	2	900	5.5	4.5	169.7	120.4	1.41
9	11	700	4.5	2.5	152.7	123.1	1.24
10	9	700	6.5	2.5	156.2	127.0	1.23
11	16	700	4.5	4.5	133.8	91.0	1.47
12	7	700	6.5	4.5	139.8	101.3	1.38
13	4	700	5.5	3.5	146.7	111.1	1.32
14	3	700	5.5	3.5	147.2	112.4	1.31
15	12	700	5.5	3.5	148.7	114.4	1.30
16	17	700	5.5	3.5	147.2	111.5	1.32
17	5	700	5.5	3.5	146.1	111.5	1.31

^a The experiment plan, as expressed in a standardized arrangement

^b The experiment plan, as actually run (in a randomized order).

Tab. 4: Design matrix and experimentally recorded data for 10 mm thickness.

Standard ^a	Run ^b	Factors			Responses		
		A (W)	B (bar)	C (m.min ⁻¹)	Upper Kerf (μm)	Lower Kerf (μm)	Ratio
1	11	1100	7	3.5	120.9	74.2	1.63
2	13	1500	7	3.5	153.4	107.3	1.43
3	17	1100	11	3.5	124.7	82.0	1.52
4	15	1500	11	3.5	177.9	134.8	1.32
5	6	1100	9	2.5	149.8	117.5	1.27
6	12	1500	9	2.5	198.4	172.5	1.15
7	9	1100	9	4.5	136.3	79.2	1.72
8	3	1500	9	4.5	165.4	116.5	1.42
9	16	1300	7	2.5	174.9	145.8	1.20
10	10	1300	11	2.5	185.2	161.0	1.15
11	7	1300	7	4.5	149.2	93.8	1.59
12	2	1300	11	4.5	160.0	113.5	1.41
13	1	1300	9	3.5	170.0	128.8	1.32
14	5	1300	9	3.5	172.3	130.5	1.32
15	8	1300	9	3.5	172.8	129.9	1.33
16	4	1300	9	3.5	171.2	130.7	1.31
17	14	1300	9	3.5	170.2	127.0	1.34

^a The experiment plan, as expressed in a standardized arrangement

^b The experiment plan, as actually run (in a randomized order).

Tab. 5: Design matrix and experimentally recorded data for 15 mm thickness.

Standard ^a	Run ^b	Factors			Responses		
		A (W)	B (bar)	C (m.min ⁻¹)	Upper Kerf (μm)	Lower Kerf (μm)	Ratio
1	12	1400	7	3.45	131.2	74.8	1.75
2	9	2000	7	3.45	168.3	123.8	1.36
3	14	1400	11	3.45	145.8	92.3	1.58
4	10	2000	11	3.45	180.4	140.9	1.28
5	4	1400	9	2.50	157.4	112.4	1.40
6	16	2000	9	2.50	208.8	168.4	1.24
7	11	1400	9	4.40	145.6	73.9	1.97
8	17	2000	9	4.40	165.5	118.2	1.40
9	5	1700	7	2.50	183.6	154.3	1.19
10	6	1700	11	2.50	197.4	174.7	1.13
11	3	1700	7	4.40	158.3	96.5	1.64
12	1	1700	11	4.40	170.4	120.9	1.41
13	15	1700	9	3.45	186.4	143.4	1.30
14	13	1700	9	3.45	185.9	141.9	1.31
15	2	1700	9	3.45	185.8	142.8	1.30
16	7	1700	9	3.45	186.1	143.5	1.30
17	8	1700	9	3.45	186.5	143.2	1.30

^a The experiment plan, as expressed in a standardized arrangement

^b The experiment plan, as actually run (in a randomized order).

Analysis of variance

To test the significance of the regression models, a test for significance on each model coefficient was carried out. The step-wise regression method was selected to automatically determine the significant model terms. The resulting nine ANOVA tables for the reduced quadratic models summarized the analysis of variance of each response and showed which model terms were significant. However, to avoid confusing the reader, these tables were abstracted to present only the most important information, as shown in Tab. 6. This table also shows the other adequacy measures: R^2 , adjusted R^2 , and predicted R^2 . All adequacy measures were close to 1 because of the high number of degrees of freedom in relation to the number of experiments (Li et al. 2014).

Tab. 6. Summary of results of ANOVA analysis.

Thickness (mm)	Response	Degrees of Freedom	Probability (F model)	R^2	Adjusted R^2	Predicted R^2
5	Upper kerf	9	<0.0001(Sig.)	0.9977	0.9948	0.9726
	Lower kerf	9	<0.0001(Sig.)	0.9982	0.9960	0.9855
	Ratio	9	<0.0001(Sig.)	0.9799	0.9540	0.7053
10	Upper kerf	9	<0.0001(Sig.)	0.9966	0.9923	0.9590
	Lower kerf	9	<0.0001(Sig.)	0.9985	0.9966	0.9872
	Ratio	9	<0.0001(Sig.)	0.9973	0.9937	0.9742

15	Upper kerf	9	<0.0001(Sig.)	0.9998	0.9995	0.9973
	Lower kerf	9	<0.0001(Sig.)	0.9943	0.9870	0.9104
	Ratio	9	<0.0001(Sig.)	0.9994	0.9987	0.9925

The final mathematical models, in terms of the coded factors, are provided by Eqs. (1) through (9) below, where A is the laser power in Watts, B is the air pressure in bar, and C is the cutting speed in $\text{m}\cdot\text{min}^{-1}$.

Eqs. (1) through (3) give mathematical models for the 5-mm-thick recombinant bamboo.

$$\begin{aligned} \text{Upper kerf} = & 147.18 + 24.67 \times A + 2.49 \times B - 9.28 \times C + 0.15 \times A \times B - 1.60 \times A \times C + 0.62 \times B \times C \\ & + 3.12 \times A^2 - 8.65 \times B^2 + 7.10 \times C^2 \end{aligned} \quad (1)$$

$$\begin{aligned} \text{Lower kerf} = & 112.19 + 24.15 \times A + 4.00 \times B - 14.56 \times C + 0.51 \times A \times B - 5.99 \times A \times C + 1.61 \times B \times C \\ & - 1.60 \times A^2 - 8.56 \times B^2 + 6.99 \times C^2 \end{aligned} \quad (2)$$

$$\begin{aligned} \text{Ratio} = & 1.31 - 0.077 \times A + 0.031 \times B + 0.086 \times C + 0.0075 \times A \times B + 0.032 \times A \times C \\ & - 0.020 \times B \times C + 0.066 \times A^2 + 0.034 \times B^2 - 0.016 \times C^2 \end{aligned} \quad (3)$$

Eqs. (4) through (6) give mathematical models for 10-mm-thick recombinant bamboo.

$$\begin{aligned} \text{Upper kerf} = & 171.31 + 20.43 \times A + 6.18 \times B - 12.17 \times C + 5.17 \times A \times B - 4.88 \times A \times C + 0.12 \times B \times C \\ & - 15.97 \times A^2 - 11.12 \times B^2 + 7.14 \times C^2 \end{aligned} \quad (4)$$

$$\begin{aligned} \text{Lower kerf} = & 129.40 + 22.27 \times A + 8.79 \times B - 24.22 \times C + 4.90 \times A \times B - 4.45 \times A \times C + 1.08 \times B \times C \\ & - 18.47 \times A^2 - 11.37 \times B^2 + 10.50 \times C^2 \end{aligned} \quad (5)$$

$$\begin{aligned} \text{Ratio} = & 1.32 - 0.10 \times A - 0.056 \times B + 0.17 \times C + 0.0001 \times A \times B - 0.044 \times A \times C - 0.033 \times B \times C + 0.10 \times A^2 \\ & + 0.049 \times B^2 - 0.035 \times C^2 \end{aligned} \quad (6)$$

Eqs. (7) through (9) give mathematical models for 15-mm-thick recombinant bamboo.

$$\begin{aligned} \text{Upper kerf} = & 186.14 + 17.88 \times A + 6.57 \times B - 13.42 \times C - 0.64 \times A \times B - 7.88 \times A \times C - 0.44 \times B \times C \\ & - 18.91 \times A^2 - 10.80 \times B^2 + 2.10 \times C^2 \end{aligned} \quad (7)$$

$$\begin{aligned} \text{Lower kerf} = & 142.97 + 24.73 \times A + 9.92 \times B - 25.04 \times C - 0.069 \times A \times B - 2.91 \times A \times C + 0.97 \times B \times C \\ & - 26.69 \times A^2 - 8.32 \times B^2 + 1.96 \times C^2 \end{aligned} \quad (8)$$

$$\begin{aligned} \text{Ratio} = & 1.30 - 0.18 \times A - 0.068 \times B + 0.18 \times C + 0.023 \times A \times B - 0.10 \times A \times C - 0.042 \times B \times C + 0.18 \times A^2 \\ & + 0.016 \times B^2 + 0.025 \times C^2 \end{aligned} \quad (9)$$

Adequacy of the developed models

The adequacy and improvements of the developed models were tested by three confirmation experiments carried out with different parameters. These experiments were selected according to the optimization results. Predicted values for the UK, LK, and their ratio were calculated for validation experiments using the point prediction option of the Design-Expert software and the mathematical models developed above. Tab. 7 presents the experimental conditions, actual experimental values, predicted values, and error for all thicknesses tested.

Tab. 7: Confirmation experiments.

Thickness (mm)	Factors			Values	Responses		
	A (W)	B (bar)	C ($\text{m}\cdot\text{min}^{-1}$)		Upper Kerf (μm)	Lower Kerf (μm)	Ratio
5	774.8	6.1	2.5	Actual	169.7	145.2	1.17
				Predicted	170.9	142.0	1.20
				Error (%)	-3.8	2.28	-6.0
10	1300.0	9.0	3.5	Actual	173.5	128.1	1.35
				Predicted	171.3	129.4	1.32
				Error (%)	3.5	-4.3	8.0
15	1700.0	9	3.5	Actual	184.1	139.3	1.32
				Predicted	186.1	143.0	1.30
				Error (%)	-1.1	-2.7	1.6

DISCUSSION

Upper kerf

Fig. 1a, b, and c show the main effects of the evaluated cutting parameters on the upper kerf response for all thicknesses tested. It is clear that the factors with the major effects on the upper kerf were the laser power and cutting speed. The upper kerf increased as the laser power increased. However, it increased as the cutting speed decreased. This was in agreement with expectations because when carrying out laser cutting slowly, more material is combusted and ejected, causing the upper kerf to increase given that more heat is introduced into the sample. Increasing the laser power increased the upper kerf due to the increase in input heat at the greater laser power. These results agree with Eltawahni et al. (2011) and Lum et al. (2000). From this graph, it is evident that the air pressure had different effects on the upper kerf for different sample thicknesses. In general, the air pressure was not a significant factor affecting the upper kerf.

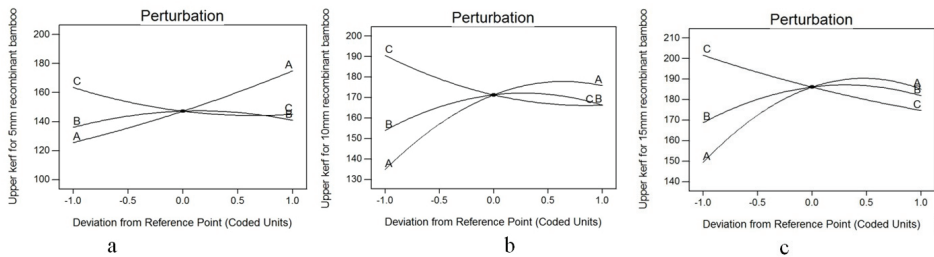


Fig. 1: Perturbation plots showing the effect of each factor on the average upper kerf for thicknesses of a) 5 mm, b) 10 mm, and c) 15 mm.

Lower kerf

Figs. 2a, b, and c show the average lower kerf widths for all thicknesses. In this plot, it is clear that the main factors affecting the lower kerf were the laser power and cutting speed. The lower kerf decreased as the cutting speed increased. Furthermore, the lower kerf increased as the laser power increased and this agrees well enough with the results found in previous studies (Eltawahni et al. 2010 and 2013). The air pressure had only a small effect on the average lower kerf for 5- and

10-mm-thick samples. In the thicker samples, the effect of air pressure was larger.

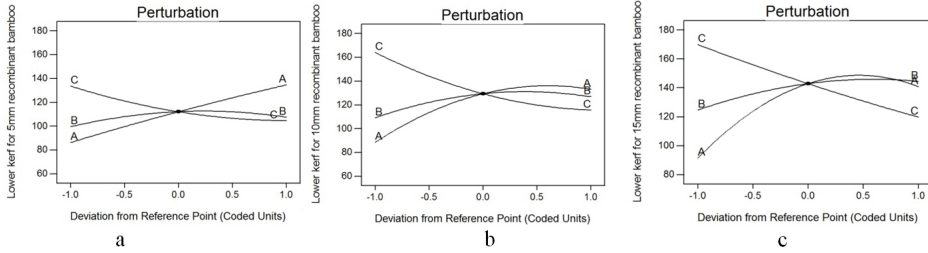


Fig. 2: Perturbation plots showing the effect of each factor on the average lower kerf for thicknesses of a) 5 mm, b) 10 mm, and c) 15 mm.

Ratio between upper kerf and lower kerf

Figs. 3a, b, and c show the effects of the evaluated cutting parameters on the ratio between the upper kerf and the lower kerf for each thickness tested. It is clear that the ratio between the upper kerf and the lower kerf was most dramatically affected by the cutting speed. This is because energy from the laser cannot instantaneously be transmitted to the lower surface of the work piece. The result has a good agreement with MDF cutting with laser beam (Eltawahni et al. 2011). The laser power had the second-largest effect on the ratio, as shown in the figure. The ratio decreased as the laser power increased. This effect became more significant as the thickness increased. The air pressure had only a slight effect on the 5- and 10-mm-thick samples, but it had a larger effect on the 15-mm-thick samples. Figs. 4a, b, and c are contour graphs showing the effect of the cutting speed and laser power on the ratio for each of the thicknesses tested. These figures are useful in identifying the area in which the ratio was minimized.

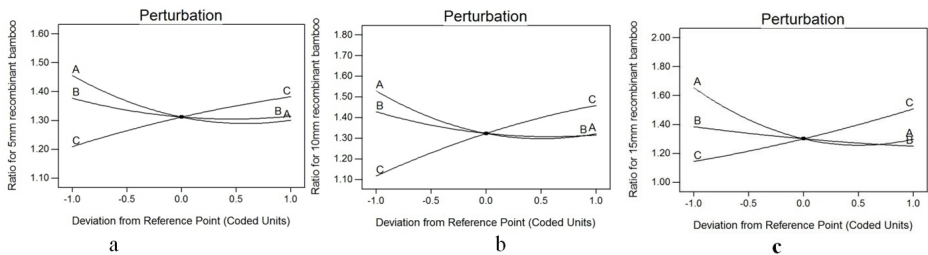
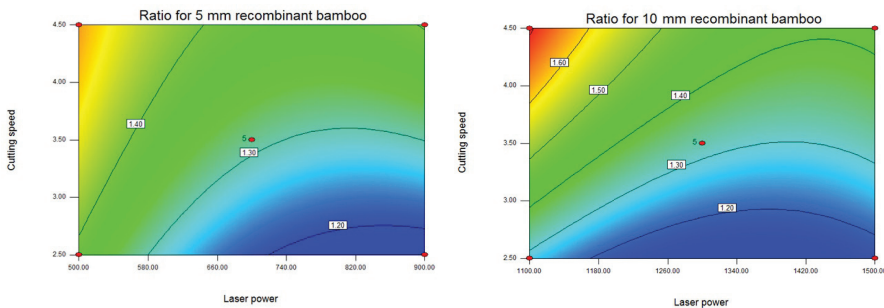


Fig. 3: Perturbation plots showing the effect of each factor on the ratio for thicknesses of a) 5 mm, b) 10 mm, and c) 15 mm.



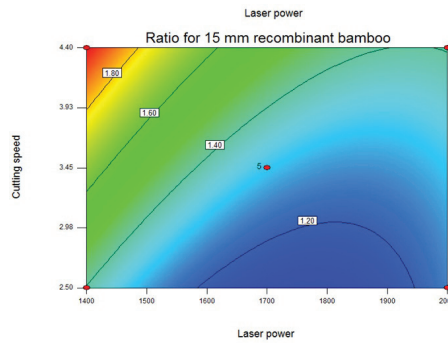


Fig. 4: Contour graphs showing the effect of laser power and cutting speed for thicknesses of a) 5 mm, b) 10 mm, and c) 15 mm.

Optimization

Cutting recombinant bamboo is a multi-factor process. Proper optimization of the parameters involved is needed to achieve high quality and optimal process efficiency. The effects of each factor (and their interactions with the other factors) on the response, as well as the output of the process, must be carefully regarded when attempting any optimization. The ratio between the upper kerf and the lower kerf is an important index which can be used to evaluate the kerf performance. The value of ratio approaching to 1 is desired in this study. The optimization criteria used in this study are shown in Tab. 8. As determined using Design-expert, the optimal solutions for each of the three thicknesses tested are shown in Tab. 9. Using these optimal solutions, it is simple to find the optimum parameters for the cutting of recombinant bamboo.

Tab. 8: Criteria for numerical optimization.

Factor or Response	Goal	Importance
Laser power	Is in range	3
Air pressure	Is in range	3
Cutting speed	Is in range	3
Upper kerf	Is in range	3
Lower kerf	Is in range	3
Ratio	Target to minimize value	5

Tab. 9: Optimal solution obtained by design-expert for the thicknesses tested.

Thickness	Number	A	B	C	Upper Kerf	Lower Kerf	Ratio	Desirability
5 mm	1	774.83	6.12	2.54	170.9	142.0	1.19	1.000
	2	822.90	6.22	2.58	175.9	146.7	1.19	1.000
	3	829.79	4.84	2.53	176.1	146.1	1.19	1.000
	4	766.92	6.17	2.50	170.1	141.5	1.19	1.000

10 mm	1	1414.13	9.67	2.67	196.7	167.6	1.15	1.000
	2	1433.02	9.49	2.65	197.9	169.0	1.15	1.000
	3	1286.01	8.27	2.55	184.0	155.9	1.15	1.000
	4	1405.41	8.00	2.55	191.0	162.9	1.15	1.000
15 mm	1	1733	11	2.50	203.3	174.6	1.13	1.000
	2	1732	10	2.50	203.5	174.7	1.13	1.000
	3	1740	11	2.50	202.8	174.7	1.13	1.000
	4	1735	11	2.50	203.3	174.7	1.13	1.000

CONCLUSIONS

Based on the experimental data reported herein, the following conclusions can be drawn:

- (1) The individual and interaction effects of all investigated factors were determined. Every factor tested can potentially affect the responses, albeit to differing degrees.
- (2) The laser power had the major effect on the upper kerf. The upper kerf increased as the laser power increased, but decreased as the cutting speed increased.
- (3) The laser power and cutting speed had the main effects on the lower kerf. The lower kerf increased as the laser power increased. However, it decreased as the cutting speed increased.
- (4) The cutting speed had the most major effect on the ratio of upper kerf-to-lower kerf. The ratio increased as the cutting speed increased. Main conclusions, concise summary of research results.

ACKNOWLEDGMENT

The authors are grateful for funding from the Priority Academic Program Development of the Jiangsu Higher Education Institutions (PAPD), the National Sci-tech Support Plan of China (No. 2012BAD24B01) and Jiangsu province ordinary university graduate student scientific research innovation projects (No. KYLX-0888).

REFERENCES

1. Barcikowski, S., Koch, G., Odermatt, J., 2006: Characterization and modification of the heat affected zone during laser material processing of wood and wood composites. *Holz als Roh- und Werkstoff* 64(2): 94-103.
2. Barnekov, V.G., McMillin, C.W., Huber, H.A., 1986: Factors influencing laser cutting of wood. *For. Prod. J.* 36(1): 55-58.
3. Eltawahni, H.A., Rossini, N.S., Dassisti, M., Alrashed, K., Aldaham, T.A., Benyounis, K.Y., Olabi, A.G., 2013: Evaluation and optimization of laser cutting parameters for plywood materials. *Optics and Lasers in Engineering* 51(9): 1029-1043.
4. Eltawahni, H. A., Olabi, A.G., Benyounis, K.Y., 2011: Investigating the CO₂ laser cutting parameters of MDF wood composite material. *Optics & Laser Technology* 43(3): 648-659.
5. Eltawahni, H.A., Olabi, A.G., Benyounis, K.Y., 2010: Effect of process parameters and optimization of CO₂ laser cutting of ultrahigh-performance polyethylene. *Mater. Des.* (8): 4029-3831.

6. Guo, X., Ekevad, M., Grönlund, A., Marklund, B., Cao, P., 2014a: Tool wear and machined surface roughness during wood flour/polyethylene composite peripheral up-milling using cemented tungsten carbide tools. *BioRes.* 9(3): 3779-3791.
7. Guo, X., Ekevad, M., Marklund, B., Li, R., Cao, P., Grönlund, A., 2014b: Cutting forces and chip morphology during wood plastic composites orthogonal cutting. *BioRes.* 9(2): 2090-2106.
8. Li, R., Ekevad, M., Wang, J., Guo, X., Cao, P., 2014: Testing and modeling of thrust force and torque in drilling recombinant bamboo. *Bioresources* 9(4): 7326-7335.
9. Lum, K.C.P., Black, I., 2000: CO₂ laser cutting of MDF. Estimation of power distribution. *J. Opt. Laser Tech.* 32(1): 77-87.
10. McMillin, C.W., Harry, J.E., 1971: Laser machining of southern pine. *For. Prod. J.* 21(10): 35-37.
11. Mukherjee, K., Grendzwell, T., Khan, P. A. A., McMillin, C.W., 1990: Gas flow parameters in laser cutting of wood-nozzle design. *For. Prod. J.* 40(10): 39-42.
12. Naderi, N., Legacey, S., Chin, S.L., 1990: Preliminary investigations of ultrafast intense laser wood processing. *For. Prod. J.* 49(6): 72-76.
13. Pires, M.C., Araujo, J.L., Teixeira, M.R., Rodrigues, F.C., 1989: Plywood inlays through CO₂ laser cutting. CO₂ laser and applications. *SPIE Proceedings* 1042: 97-102.
14. Wang, S.G., Hua, Y.K., 1991: The research of recombinant bamboo manufacturing technology. *Wood industry* 5(2): 14-19.
15. Yang, Y.F., 2005: Study on cutting performance of bamboo. *Journal of Beijing Forestry University* 10(5): 35-45.
16. Zhao, R.J., Yu, Y.S., 2002: The technology of artificial bamboo board. China Forestry Press, Beijing.

RONGRONG LI, XIAOLEIGUO, PINGXIANG CAO*
 NANJING FORESTRY UNIVERSITY
 FACULTY OF MATERIAL SCIENCE AND ENGINEERING
 NANJING
 JIANGSU
 CHINA

Corresponding author: caopx@njfu.com.cn, lirr722@hotmail.com

XIAODONG(ALICE) WANG
 LULEÅ UNIVERSITY OF TECHNOLOGY, DIVISION OF WOOD SCIENCE
 AND ENGINEERING
 SKELLEFTEÅ
 SWEDEN

